Supplemental Materials

Furoxans (1, 2, 5 Oxadiazole-N-Oxides) as Novel NO Mimetic Neuroprotective and Procognitive Agents

Isaac T. Schiefer[†], *Lawren VandeVrede*[†], *Mauro Fa'*[‡], *Ottavio Arancio*[‡] *and Gregory R. J. Thatcher*[†,*]

[†]Department of Medicinal Chemistry and Pharmacognosy, College of Pharmacy, University of Illinois at Chicago, 833 S. Wood St., Chicago, IL 60612-7231

[‡]Department of Pathology, The Taub Institute for Research on Alzheimer's Disease and the Aging Brain, Columbia University, P&S #12-420D, 630W 168th St., New York, NY 10032

E-mail: thatcher@uic.edu

* To whom correspondence about the manuscript should be sent: Department of Medicinal Chemistry and Pharmacognosy, College of Pharmacy, University of Illinois at Chicago (MC 781), 833 S. Wood St., Chicago, IL 60612-7231. Tel: 312-355-5282. Fax: 312 996 7107.

List of Contents

Cysteine depletion with furoxans

The appropriate furoxan (250 μM) was dissolved in a solution of PBS (50 mM, pH 7.4, /CH_3CN (1:1); and L-cysteine (2.5 mM) was added followed by incubation at 37 °C for 4 h. Aliquots were analyzed by mixing with DTNB solution [750 μM, in PBS 50 mM, pH 7.0]) for 5 min. UV absorbance of DTNB mixture was measured at 412 nm using a Dynex MRX II microplate spectrophotometer and calibrated using a standard curve constructed using L-cysteine in the presence of DTNB to yield total reduced cysteine concentration. Values were plotted against time and showed significant background cysteine oxidation in the absence of furoxans (Figure S1). Observed rate constants were calculated using a nonlinear first order rate decay and are listed within Figure S1. Additional experiments were therefore carried out under hypoxic conditions, and in the presence of metal ion chelators to discourage redox metal facilitated oxidation with scarce amounts of O_2 (described in experimental portion of manuscript).

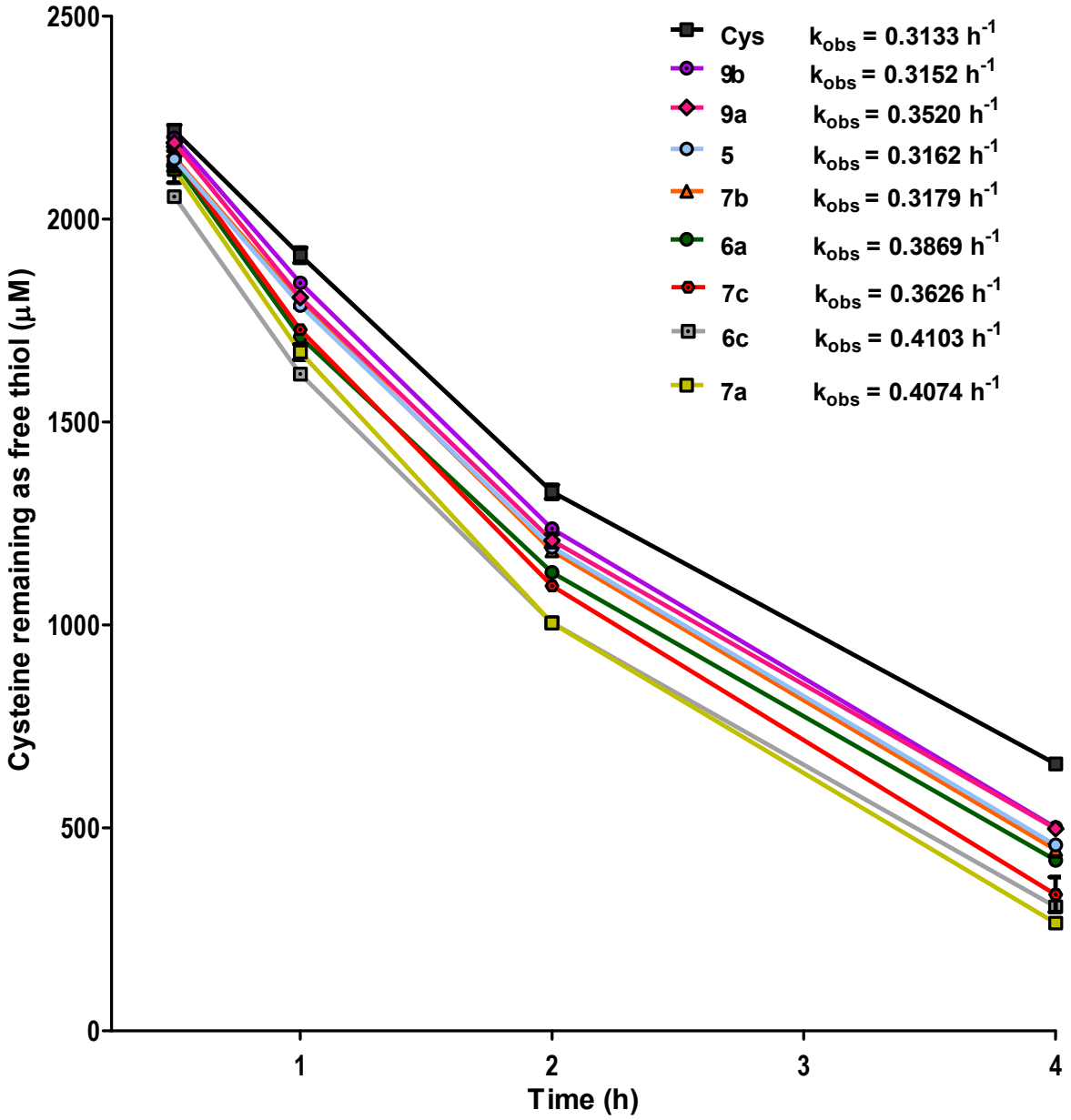

Figure S1. Cysteine remaining as free thiol upon incubation of cysteine (2.5 mM) with the appropriate furoxan (250 µM) for 4 h under normoxic conditions at 37 °C in PBS (50 mM, pH 7.4)/ CH_3CN (1:1), with 1 mM EDTA. Reduced cysteine quantified using UV absorbance following treatment with DTNB solution.

Nitrite Production from Furoxans

The parent furoxan (250 μM) was dissolved in PBS (50 mM, pH 7.4)/CH_3CN (1:1); L-cysteine (2.5 mM) was added and the mixture incubated at 37 °C for 24 h. Aliquots (taken at 1, 2, 4, 8, 12, 18 & 24 h) were incubated for 10 min with griess reagent A (1.0 % sulfanilamide, 5.0 % H_3PO_4 in dH_2O)/ griess reagent B (0.1 % (N-1-naphthyl)ethylenediamine dihydrochloride in dH_2O). UV absorbance at 530 nm was measured using a Dynex MRX II microplate spectrophotometer and calibrated using a standard curve constructed with $NaNO_2$ to yield nitrite concentration. Furoxans were found to give maximum NO_2^- generation within 24 h. Addition of L-cysteine (1000 uM) after 24 h gave no increase in NO_2^- generation, ruling out the possibility of complete cysteine oxidation being responsible for lack of NO_2^-generation beyond 24 h. A full time course was not acquired for **6b** and **7c**, as the 18 & 24 h time points were sufficient for our purposes.

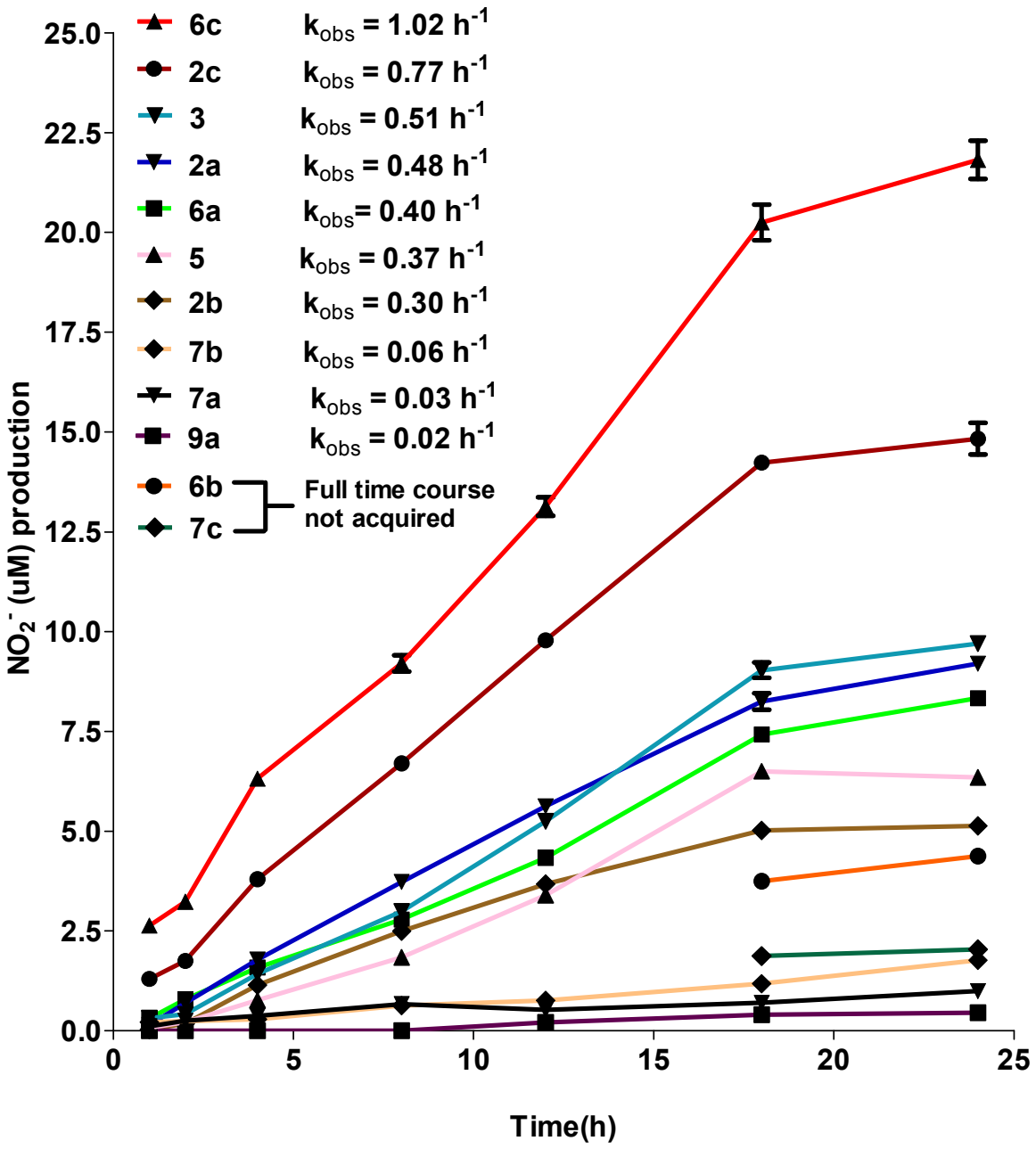

Figure S2. Time course of nitrite production upon incubation of cysteine (2.5 mM) with the appropriate furoxan (250 μM) at 37 °C in PBS (50 mM, pH 7.4). Aliquots were analyzed at (1, 2, 4, 8, 12, 18, and 24 h). Observed rate constants calculated using linear regression analysis of 1-18 h time points.

Mechanistic Reactivity Analysis

Reactivity of the furoxans were assessed via incubation of the appropriate furoxan (75 μM) with L-cysteine (2.5 mM) in phosphate buffer (50 mM, pH 7.4) at 37 °C for 2 h. The products were then separated and analyzed by HPLC-MS/MS. Peak integration from UV absorbance (λ = 250 nm) spectra gave the relative abundance of each reaction product, and was correlated with the TIC chromatogram to identify peaks by MS/MS analysis.

Analysis of Reaction of 6a with L-cysteine

After 2 h in the presence of excess cysteine, **6a** yielded three main reaction products, and tentative structures have been assigned based on the observed m/z values (Figure S2). Approximately 72 % of **6a** remained after 2 h, and no cysteine adduct was observed. One of the three major products, **E** (~8-12 %), was found to be the likely end product NO_x release. Interestingly, it appears that **E** is present as a mixture of isomers, which have the same m/z values but slightly different retention times. The relative formation of **E** from **6a** (~8-12 %) corresponds well with the observe NO_2^- production of **6a** (~13 % mol/mol), and helps support formation of **E** as indicative of NO_x release from this molecule.

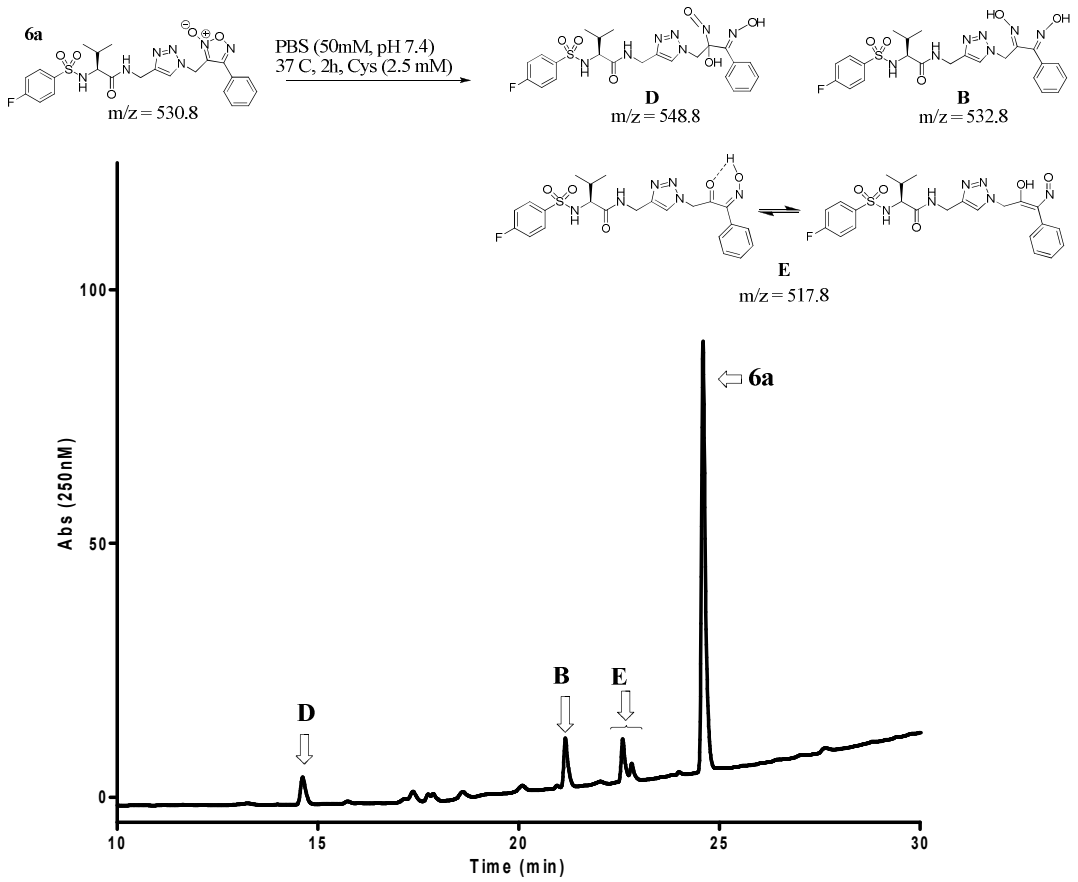

Figure S2. HPLC-UV$_{(\lambda = 250nm)}$ chromatogram of the reaction between **6a** (75 μM) with L-cysteine (2.5 mM) in phosphate buffer (50 mM, pH 7.4) at 37 °C for 2 h. Peaks identified by LC-MS/MS analysis.

Analysis of Reaction of 6c with L-cysteine

The relatively high and complex reactivity of **6c** compared to the other furoxans studied is easily noticed upon examination of the reaction profiles by HPLC-MS/MS (Figure S3). **6c** gave some products that were not seen for any of the other derivatives studied, namely products **I** & **II**. **I** (~ 5 %) corresponds to a product likely resulting from the peptidomimetic triazole **I** acting as a stable leaving group. **II** represents a hydroxylamine containing molecule which represents ~55 % of total products, presumably formed as the result of a highly energetic intermediate that results in the breaking apart of the furoxan ring itself. **I** and **II** are speculated to be responsible

for the large amounts of NO_2^- observed from **6c** in the griess assay. The NO_x releasing product (**E**) only represents approximately 10 % of the entire reaction products. In the manuscript, **6c** was omitted from the correlation of NO_2^- versus neuroprotection due to the atypical NO_2^- production observed; however, if considering the relative amount of **E** as indicative of NO_x release, **6c** would fit adequately into our correlation for NO_x and neuroprotection. These findings signify the complex and high reactivity of **6c**, and support our hypothesis that in this circumstance, NO_2^- generation does not correlate with biologically relevant NO_x produced.

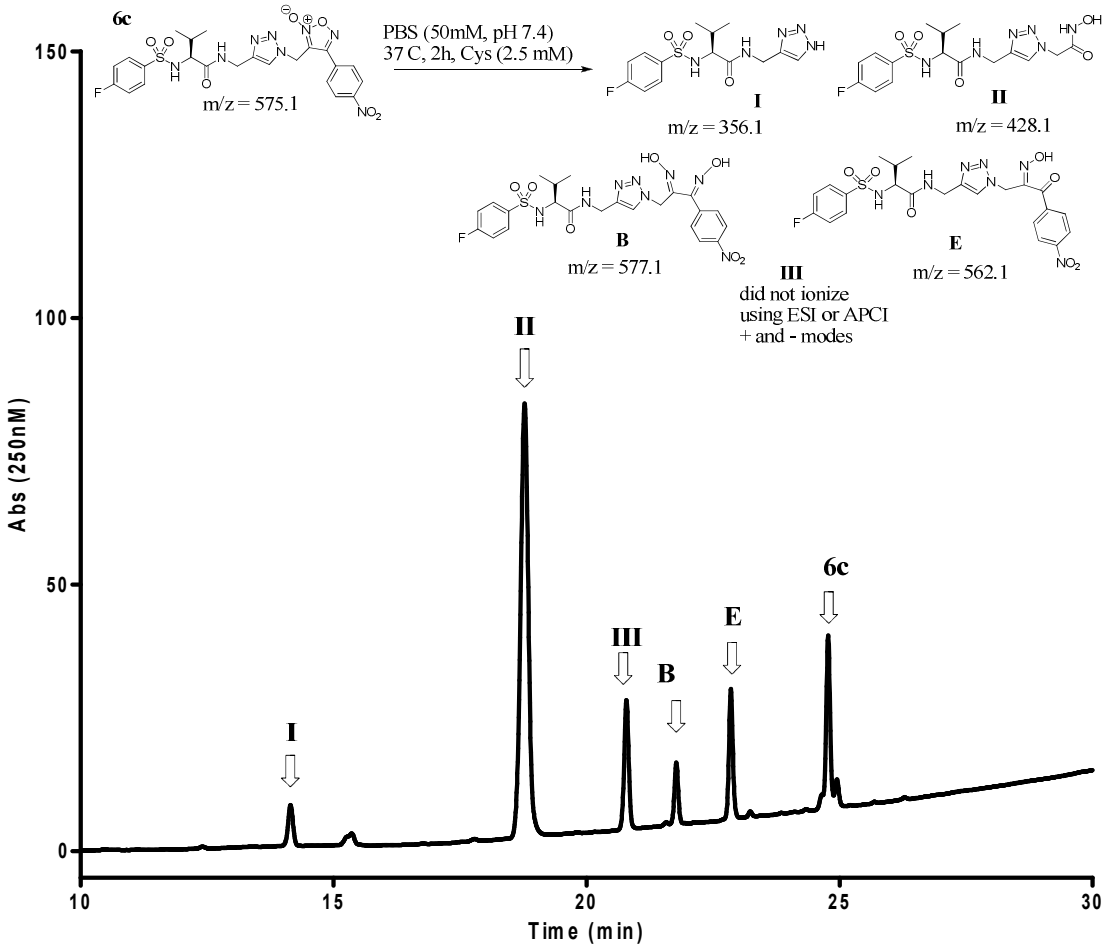

Figure S3. HPLC-UV$_{(\lambda = 250nm)}$ chromatogram of the reaction between **6c** (75 μM) with L-cysteine (2.5 mM) in phosphate buffer (50 mM, pH 7.4) at 37 °C for 2 h. Peaks identified by LC-MS/MS analysis.

^{18}O-incoporation Studies

The following mechanistic ^{18}O-incoporation data was excluded from the original manuscript because it tended to detract from the flow and focus of the text; however, the results are novel and noteworthy for those interested in furoxan mechanistic chemistry.

To gain further mechanistic understanding about the formation and existence of the keto-oxime product (**E**), we performed isotope labeling studies utilizing $H_2{}^{18}O$.Incubations were carried out similarly to those used for mechanistic analysis, with the implementation of $H_2{}^{18}O$. **6c** or **7c** (150 μM) were incubated in equal volumes of PBS (50 μM, pH 7.4)/ H_2O or $H_2{}^{18}O$ in the presence of excess cysteine (5 mM) at 37 °C for 2 h. Reaction aliquots were analyzed by HPLC-MS/MS (Figure S4). Control experiments containing the naturally abundant ^{16}O afforded the aforementioned keto-oxime product, **E** (**6c**, Figure S4-A; **7c**, Figure S4-C), with a $[M+H^+]$ of 562.2 m/*z*. Interestingly, we observed implementation of ^{18}O into the product corresponding to **E** (**6c**, Figure S4-B; **7c**, Figure S4-D), with a mass of 564.2 m/z. The ratio of ^{16}O:^{18}O incorporated in **E** was proportional to the relative amounts of PBS/H_2O or $H_2{}^{18}O$, approximately 1:1. These results clearly demonstrate that the -OH in **E** originates from H_2O, and not from molecular O_2, or a complex and unlikely rearrangement of the parent N-Oxide moiety itself. Despite the distinctive differences in the reactivity of **6c** and **7c**, the incorporation of ^{18}O into **E** is equivalent in both instances, suggesting a common mechanistic pathway leading to the formation of the keto oxime product, and correspondingly, NO_x related biological activity.

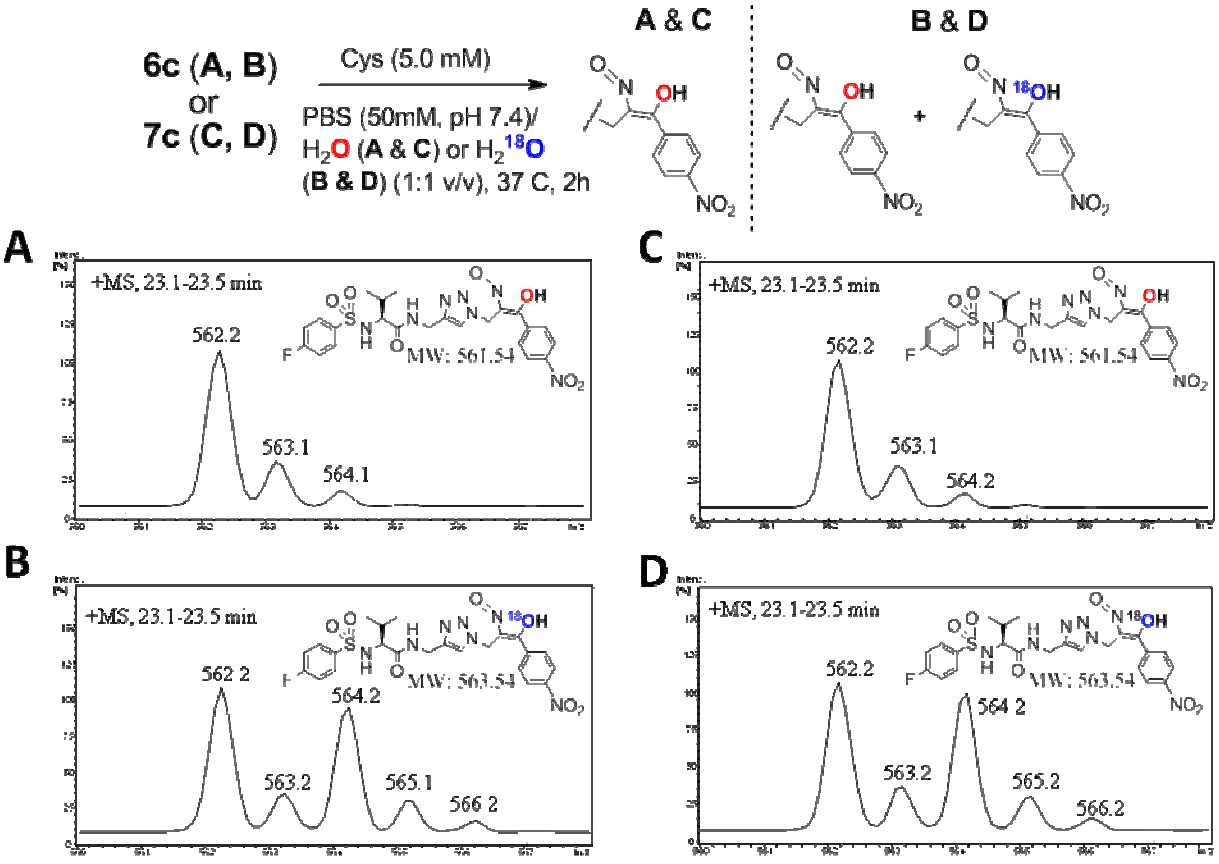

Figure S4. Mass spectrum demonstrating incorporation of ^{18}O into **III** (ESI (+) mode). **6c** (150 µM) incubated with cysteine in PBS (50 µM, pH 7.4)/ H_2O (**A**) or $H_2{}^{18}O$ (**B**) (1:1 [v/v]) for 2 h at 37 °C. **7c** (150 µM) incubated with cysteine in PBS (50 µM, pH 7.4)/ H_2O (**C**) or $H_2{}^{18}O$ (**D**) (1:1 [v/v]) for 2 h at 37 °C.

Additional Synthetic Protocols

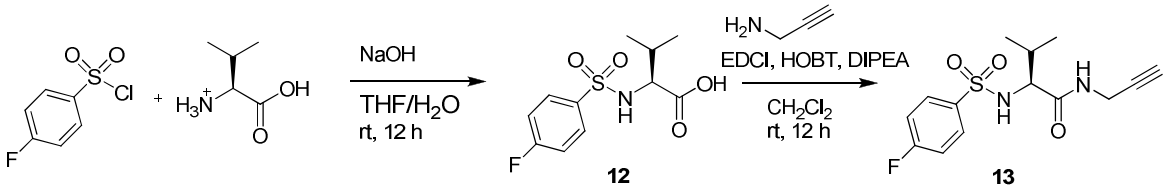

(S)-2-(4-Fluorophenylsulfonamido)-3-methylbutanoic acid (12).

4-fluorobenzenesulfonyl chloride (1.0 g, 8 mmol in THF [8 ml]) was added dropwise for 10 min to a solution of L-valine (1.0 g, 8 mmol) in 1 M NaOH (21 ml) at 0 °C. The reaction was allowed to warm to room temperature and stirred for 12 h. The reaction mixture was then acidified to pH ~ 2 using 1 M HCl, and the resulting aqueous solution extracted with ethyl acetate (3 x 75 ml). The combined organic extracts were washed with brine (2 x 30 ml), dried over Na_2SO_4 and concentrated under vacuum to give a white solid. Column chromatography (hexane/ethyl acetate [1:3]) gave the desired product as a white solid (1.46 g, 66.3 %). ^{1}H NMR (DMSO-d^6, 400 MHz): δ 12.60 (bs, 1H); 8.08-8.06 (d, 1H, J = 8.4 Hz); 7.85-7.80 (q, 2H); 7.41-7.36 (t, 2H); 3.56-3.50 (t, 1H); 2.00-1.90 (m, 1H); 0.83-0.80 (dd, 6H). ^{13}C NMR (DMSO-d^6, 100 MHz): 172.52, 165.67, 163.18, 138.01(d, J = 3.0 Hz), 130.04, 129.94, 116.49, 116.27, 61.69, 30.77, 19.44, 18.22.

(S)-2-(4-Fluorophenylsulfonamido)-3-methyl-N-(prop-2-ynyl)butanamide (13). A round bottom was charged with **12** (2.1 g, 7.6 mmol), EDCI (1.8 g, 9.2 mmol), HOBT (1.2 g, 9.2 mmol) in DMF (10 ml) at 0 °C. A separately prepared mixture of propargyl amine (420 mg, 7.62 mmol), and DIPEA (6.0 ml, 38 mmol) was added dropwise to the activated acid at 0 °C. The mixture was allowed to warm to room temperature and stir for 8 h. The mixture was then diluted

with ice water (100 ml), and extracted with ethyl acetate (3 x 150 ml). The combined organic extracts were washed with brine (2 x 50 ml), dried over Na_2SO_4 and concentrated to give a crude yellow solid which was purified by column chromatography (hexane/ethyl acetate (8:1 → 4:1) to give the desired product as a white solid (1.62 g, 68.0 %). ^{1}H NMR (MeOD-d^4, 400 MHz): δ 7.88-7.85 (q, 2H); 7.27-7.23 (t, 2H); 3.75-3.59 (qd, 2H); 3.47-3.45 (d, 1H); 2.56-2.53 (m, 1H); 1.92-1.84 (m, 1H); 0.94-0.77 (dd, 6H). ESI-HRMS (m/z): $[M+H]^+$ calcd. for $C_{14}H_{17}FN_2O_3S$: 313.0968, observed: 313.1003. $[M-H]^+$ calcd. for $C_{14}H_{17}FN_2O_3S$: 311.0919, observed: 311.0885.

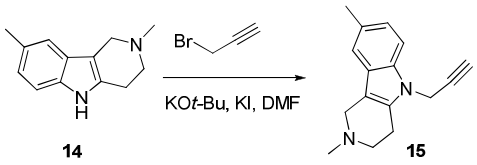

2,8-Dimethyl-5-(prop-2-ynyl)-2,3,4,5-tetrahydro-1H-pyrido[4,3-b]indole (15). Potassium *tert*-butoxide (152 mg, 1.35 mmol) in DMF (2 ml) was added dropwise to a stirred solution of the carbazole, **14**, (270 mg, 1.35 mmol [synthesized following published procedures][1]) in DMF (5 ml). After 15 min propargyl bromide (210 mg, 1.45 mmol) and KI (8 mg) were added and the reaction brought to 80 °C for 12 h. After cooling to rt, the reaction was diluted w/H_2O (30 ml), extracted w/ethyl acetate (3 x 50 ml). Combined organic extracts were dried over Na_2SO_4 and concentrated to give a crude red oil, which was purified by column chromatography to give the product as yellow solid (195 mg, 60.6 %). ^{1}H NMR (400MHz, CDCl3): 7.27-7.25 (d, 1H, J = 8.59Hz); 7.22 (s, 1H); 7.05-7.03 (d, 1H, J = 8.19Hz); 4.749-4.743 (d, 2H, J = 2.36Hz); 3.67 (s, 2H); 2.92-2.87 (m, 4H); 2.58 (s, 3H); 2.46 (s, 3H); 2.25-2.24 (t, 1H). 13C NMR (100MHz, CDCl3): 134.26, 132.49, 128.27, 125.89, 122.18, 117.28, 108.25, 108.18, 78.02, 71.75, 51.99, 51.32, 45.31, 31.90, 22.29, 21.05.

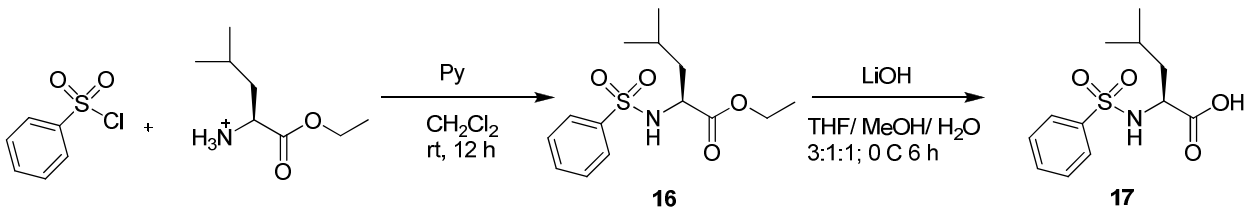

(S)-Ethyl 4-methyl-2-(phenylsulfonamido)pentanoate (16). *L*-Leucine ethyl ester hydrochloride (1 g, 5.11 mmol) was dissolved in CH_2Cl_2 and pyridine (1.6 µL, 15.3 mmol) and reaction brought to 0 °C. Benzenesulfonyl chloride (654 µL, 5.11 mmol) was then added dropwise and reaction stirred for 12 hr at rt. The reaction mixture was concentrated and purified by column chromatography (hexane/ethyl acetate [10:1]) to give the desired product as a light yellow solid (1.25g, 85.7 %). ^{1}H NMR ($CDCl_3$, 400 MHz): δ 7.87-7.85 (d, 2H, J = 8.8 Hz); 7.60-7.49 (m, 3H); 5.05-5.02 (d, 1H, J = 10.0 Hz); 3.97-3.93 (m, 1H); 3.91-3.88 (q, 2H); 1.86-1.78 (m, 1H); 1.58-1.46 (t, 2H); 1.10-1.07 (t, 3H); 0.93-0.90 (t, 6H). ^{13}C NMR ($CDCl_3$, 100 MHz): 171.52, 140.87, 132.45, 129.04, 126.46, 60.53, 54.03, 40.66, 23.84, 22.46, 21.02, 13.77.

(S)-4-Methyl-2-(phenylsulfonamido)pentanoic acid (17). 17 (600 mg, 2 mmol) was dissolved in THF/MeOH/H_2O (6 ml: 2 ml: 1 ml) and brought to 0 °C. LiOH (100 mg, 4 mmol) was then added in on portion and reaction allowed to warm to room temperature, monitored by TLC. After 4 h the reaction was diluted with ice water, and washed with ethyl acetate (2 x 50 ml). The aqueous layer was then acidified to pH ~ 2 using 1 N HCl. Aqueous layer was extracted with ethyl acetate (3 x 75 ml), followed by washing combined organic layers with brine (2 x 30 ml). Organic layer was dried over Na_2SO_4 and concentrated to give the pure acid without further purification (286 mg, 50.1 %) ^{1}H NMR ($CDCl_3$, 400 MHz): 7.85-7.83 (d, 2H, J = 8.8 Hz); 7.54-7.47 (m, 3H); 6.87 (bs, 1H); 5.12 (bs, 1H); 3.98-3.89 (m, 1H); 1.72-1.65 (m, 1H); 1.50-1.48 (m,

2H); 0.85-0.74 (dd, 6H). ^{13}C NMR ($CDCl_3$, 100 MHz): 173.26, 141.10, 132.35, 129.01, 126.48, 54.16, 41.06, 30.73, 23.88, 22.65, 21.10.

Crystallography

The furoxan (**6c**) was chosen for crystallographic examination. Molecular formula: $C_{23}H_{23}FN_8O_7S$, formula weight: 1149.11, crystal system: Orthorhombic, $P2_12_12_1$ (#19) with unit cell dimensions: a = 11.334 (1) Å b = 21.427 (2) Å, c = 21.643 (1) Å, Volume = 5256.1 (6) Å^3; Z, calculated density = 8, 1.452 Mg/m^3, Absorption coefficient = 0.190 mm^{-1}. A colorless needle, with dimensions 2 × 2 × 40 μm, was selected for data collection. The crystal was cooled to 100 K and aligned in the x-ray beam at sector 22 (SER-CAT) on the ID beamline at the Advanced Photon Source at Argonne National Lab. Data collection was carried out at a wavelength of 0.80 Å using 5° rotations and exposure time of 1 sec, and collected with a MAR 300 mm CCD detector. 72 images were indexed and integrated using XDS, and averaged over mmm symmetry. The structure was solved using SHELX-97, and refined using WinGX and SHELXL; ORTEP was used to generate the molecular figures. Hydrogen atoms were added to the model in idealized positions. The final model gave agreement factors (R indices) of R1 = 0.0407, wR2 = 0.1030. We observed two independent molecules in the asymmetric unit, confirming the presence of the oxadiazole-2-oxide structure within the structures.

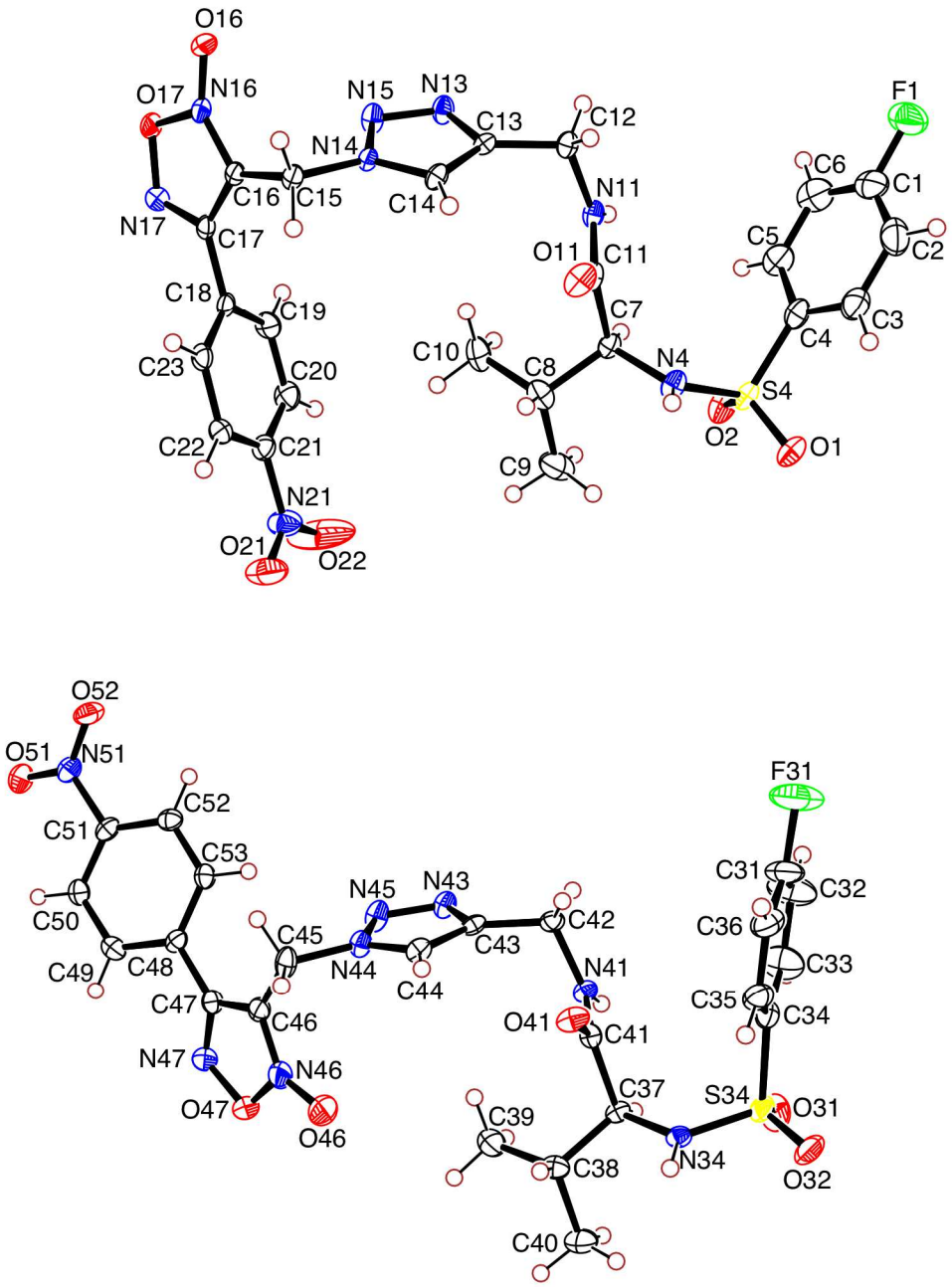
O16
O17
N16
N15
N13
F1
C13
C12
N14
C6
C1
C16
C15
C14
N11
N17
C17
C5
C2
O11
C11
C18
C19
C7
C4
C3
C10
C8
N4
C23
C20
S4
O2
O1
C22
C21
C9
N21
O21
O22
O52
O51
N51
F31
C52
C51
C31
C32
C53
N45
N43
C50
C45
C42
C36
C33
C49
C48
N44
C43
N41
C35
C34
C47
C46
C44
O41
C41
N47
N46
C37
S34
O31
O47
C39
O46
N34
C38
O32
C40

Table S1. Summary from Data Collection and Structure Refinement

Crystal Parameters	
crystal system	Orthorhombic
space group	$P2_12_12_{1(}$#19)
a (Å)	11.334(1)
b (Å)	21.427(2)
c (Å)	21.643(1)
Data Collection Statistics	
# of measured reflections	56827
# of unique reflections	9831
Completeness (%)	98.3 %
Refinement Statistics	
Resolution Range (Å)	1.51 to 29.22°
Refinement method	Full-matrix least-squares on F^2
Goodness-of-fit on F^2	1.089
Final R indices [I>2(I)]	R1 = 0.0407, wR2 = 0.1030

Table S2. Atomic coordinates ($\times 10^4$) and equivalent isotropic displacement parameters ($Å^2 \times 10^3$) for UIC09010 (**6c**). U(eq) is defined as one third of the trace of the orthogonalized U_{ij} tensor.

	X	Y	Z	U(eq)
F(1)	6951(2)	6031(1)	9935(1)	56(1)
C(1)	7239(3)	6620(2)	9755(1)	39(1)
C(2)	8407(3)	6752(2)	9667(2)	41(1)
C(3)	8711(3)	7347(1)	9458(1)	33(1)
C(4)	7834(3)	7780(1)	9355(1)	26(1)
C(5)	6650(3)	7631(2)	9463(1)	33(1)
C(6)	6353(3)	7038(2)	9664(2)	41(1)
S(4)	8205(1)	8527(1)	9072(1)	21(1)
O(1)	9430(2)	8623(1)	9205(1)	28(1)
O(2)	7344(2)	8956(1)	9301(1)	30(1)
N(4)	8081(2)	8514(1)	8330(1)	21(1)
C(7)	6922(2)	8572(1)	8031(1)	18(1)
C(8)	6887(2)	9134(1)	7587(1)	25(1)

C(9)	7251(3)	9728(1)	7919(2)	37(1)
C(10)	5661(3)	9191(1)	7302(1)	32(1)
C(11)	6669(2)	7976(1)	7672(1)	18(1)
O(11)	7349(2)	7805(1)	7259(1)	26(1)
N(11)	5688(2)	7672(1)	7801(1)	18(1)
C(12)	5298(2)	7155(1)	7408(1)	19(1)
C(13)	4804(2)	7385(1)	6811(1)	15(1)
N(13)	3625(2)	7441(1)	6720(1)	21(1)
C(14)	5362(2)	7586(1)	6286(1)	18(1)
N(14)	4490(2)	7752(1)	5902(1)	15(1)
C(15)	4581(2)	7975(1)	5258(1)	17(1)
N(15)	3431(2)	7666(1)	6160(1)	21(1)
C(16)	3509(2)	8323(1)	5074(1)	16(1)
N(16)	2585(2)	8030(1)	4840(1)	19(1)
O(16)	2353(2)	7483(1)	4723(1)	25(1)
C(17)	3205(2)	8962(1)	5089(1)	16(1)
N(17)	2145(2)	9061(1)	4872(1)	22(1)
O(17)	1700(2)	8487(1)	4704(1)	21(1)
C(18)	3921(2)	9487(1)	5322(1)	18(1)
C(19)	3642(2)	9761(1)	5886(1)	23(1)
C(20)	4322(3)	10245(1)	6109(1)	26(1)
C(21)	5251(2)	10458(1)	5761(1)	21(1)
C(22)	5545(2)	10203(1)	5198(1)	21(1)
C(23)	4880(2)	9705(1)	4981(1)	20(1)
N(21)	5972(2)	10970(1)	6002(1)	33(1)
O(21)	6817(2)	11147(1)	5710(1)	48(1)
O(22)	5702(3)	11190(2)	6500(2)	91(1)
F(31)	550(2)	324(1)	6022(1)	67(1)
C(31)	522(3)	645(2)	6574(2)	42(1)
C(32)	-408(4)	553(2)	6955(2)	56(1)

C(33)	-412(3)	862(2)	7519(2)	45(1)
C(34)	524(3)	1241(1)	7668(1)	24(1)
C(35)	1446(3)	1333(1)	7257(1)	29(1)
C(36)	1442(3)	1026(2)	6699(1)	32(1)
S(34)	630(1)	1603(1)	8401(1)	23(1)
O(31)	-370(2)	1430(1)	8759(1)	40(1)
O(32)	1793(2)	1460(1)	8620(1)	36(1)
N(34)	600(2)	2345(1)	8298(1)	18(1)
C(37)	-484(2)	2680(1)	8115(1)	16(1)
C(38)	-324(2)	3376(1)	8280(1)	23(1)
C(39)	-1364(3)	3761(1)	8065(1)	32(1)
C(40)	-138(3)	3448(2)	8972(1)	38(1)
C(41)	-724(2)	2613(1)	7421(1)	17(1)
O(41)	35(2)	2732(1)	7038(1)	24(1)
N(41)	-1817(2)	2441(1)	7273(1)	18(1)
C(42)	-2207(2)	2436(1)	6629(1)	19(1)
C(43)	-2667(2)	3060(1)	6430(1)	17(1)
N(43)	-3837(2)	3175(1)	6374(1)	21(1)
C(44)	-2076(2)	3603(1)	6299(1)	20(1)
N(44)	-2924(2)	4023(1)	6178(1)	20(1)
N(45)	-4005(2)	3768(1)	6219(1)	25(1)
C(45)	-2819(2)	4682(1)	6010(1)	25(1)
C(46)	-3518(2)	5085(1)	6436(1)	23(1)
N(46)	-3133(2)	5173(1)	7001(1)	33(1)
O(46)	-2279(2)	4966(1)	7294(1)	50(1)
C(47)	-4562(2)	5444(1)	6378(1)	22(1)
N(47)	-4797(2)	5748(1)	6889(1)	29(1)
O(47)	-3917(2)	5596(1)	7306(1)	36(1)
C(48)	-5360(2)	5500(1)	5844(1)	19(1)
C(49)	-5976(2)	6057(1)	5751(1)	24(1)

C(50)	-6708(2)	6128(1)	5245(1)	22(1)
C(51)	-6817(2)	5629(1)	4840(1)	20(1)
C(52)	-6260(2)	5067(1)	4934(1)	21(1)
C(53)	-5533(2)	5005(1)	5441(1)	20(1)
N(51)	-7530(2)	5713(1)	4275(1)	23(1)
O(51)	-8172(2)	6169(1)	4239(1)	32(1)
O(52)	-7439(2)	5314(1)	3871(1)	31(1)

Table S3. Bond lengths [Å] and angles [°] for UIC09010.

F(1)-C(1)	1.362(4)	F(31)-C(31)	1.377(4)
C(1)-C(6)	1.360(5)	C(31)-C(36)	1.352(5)
C(1)-C(2)	1.366(5)	C(31)-C(32)	1.354(5)
C(2)-C(3)	1.396(5)	C(32)-C(33)	1.388(5)
C(3)-C(4)	1.379(4)	C(33)-C(34)	1.374(4)
C(4)-C(5)	1.399(4)	C(34)-C(35)	1.387(4)
C(4)-S(4)	1.764(3)	C(34)-S(34)	1.770(3)
C(5)-C(6)	1.383(5)	C(35)-C(36)	1.374(4)
S(4)-O(2)	1.431(2)	S(34)-O(32)	1.434(2)
S(4)-O(1)	1.432(2)	S(34)-O(31)	1.423(2)
N(4)-C(7)	1.470(3)	N(34)-C(37)	1.478(3)
C(7)-C(11)	1.521(3)	C(37)-C(41)	1.533(3)
C(7)-C(8)	1.542(3)	C(37)-C(38)	1.545(4)
C(8)-C(9)	1.520(4)	C(38)-C(39)	1.512(4)
C(8)-C(10)	1.525(4)	C(38)-C(40)	1.519(4)
C(11)-O(11)	1.236(3)	C(41)-O(41)	1.223(3)
C(11)-N(11)	1.319(3)	C(41)-N(41)	1.332(3)
N(11)-C(12)	1.465(3)	N(41)-C(42)	1.463(3)
C(12)-C(13)	1.492(3)	C(42)-C(43)	1.499(4)
S(4)-N(4)	1.611(2)	S(34)-N(34)	1.605(2)
C(13)-N(13)	1.356(3)	C(43)-N(43)	1.354(3)
C(13)-C(14)	1.372(4)	C(43)-C(44)	1.372(4)
N(13)-N(15)	1.323(3)	N(43)-N(45)	1.327(3)
C(14)-N(14)	1.339(3)	C(44)-N(44)	1.342(3)
N(14)-N(15)	1.336(3)	N(44)-N(45)	1.345(3)
N(14)-C(15)	1.477(3)	N(44)-C(45)	1.464(3)
C(15)-C(16)	1.481(3)	C(45)-C(46)	1.491(4)

C(16)-N(16)	1.321(3)	C(46)-N(46)	1.312(4)
C(16)-C(17)	1.412(4)	C(46)-C(47)	1.417(4)
N(16)-O(16)	1.229(3)	N(46)-O(46)	1.239(3)
N(16)-O(17)	1.432(3)	N(46)-O(47)	1.432(3)
C(17)-N(17)	1.307(3)	C(47)-N(47)	1.311(4)
C(17)-C(18)	1.477(3)	C(47)-C(48)	1.472(4)
N(17)-O(17)	1.378(3)	N(47)-O(47)	1.385(3)
C(18)-C(19)	1.389(4)	C(48)-C(49)	1.397(4)
C(18)-C(23)	1.394(4)	C(48)-C(53)	1.386(4)
C(19)-C(20)	1.381(4)	C(49)-C(50)	1.383(4)
C(20)-C(21)	1.373(4)	C(50)-C(51)	1.387(4)
C(21)-C(22)	1.376(4)	C(51)-C(52)	1.376(4)
C(21)-N(21)	1.465(4)	C(51)-N(51)	1.476(3)
C(22)-C(23)	1.390(4)	C(52)-C(53)	1.380(4)
N(21)-O(21)	1.208(3)	N(51)-O(51)	1.220(3)
N(21)-O(22)	1.216(3)	N(51)-O(52)	1.228(3)

Table S4. Bond angles [°] for UIC09010 (**6c**).

C(6)-C(1)-F(1)	118.4(3)	C(36)-C(31)-F(31)	117.2(3)
F(1)-C(1)-C(2)	117.6(3)	C(32)-C(31)-F(31)	118.3(3)
C(6)-C(1)-C(2)	124.0(3)	C(36)-C(31)-C(32)	124.5(3)
C(1)-C(2)-C(3)	118.3(3)	C(31)-C(32)-C(33)	118.0(3)
C(4)-C(3)-C(2)	119.2(3)	C(34)-C(33)-C(32)	119.1(3)
C(3)-C(4)-C(5)	120.7(3)	C(33)-C(34)-C(35)	121.0(3)
C(3)-C(4)-S(4)	119.6(2)	C(33)-C(34)-S(34)	121.5(2)
C(5)-C(4)-S(4)	119.7(2)	C(35)-C(34)-S(34)	117.5(2)
C(6)-C(5)-C(4)	119.7(3)	C(36)-C(35)-C(34)	119.6(3)
C(1)-C(6)-C(5)	118.1(3)	C(31)-C(36)-C(35)	117.8(3)
O(2)-S(4)-O(1)	119.89(12)	O(31)-S(34)-O(32)	119.73(13)
O(2)-S(4)-N(4)	107.26(12)	O(32)-S(34)-N(34)	106.09(13)
O(1)-S(4)-N(4)	106.75(12)	O(31)-S(34)-N(34)	108.45(13)
O(2)-S(4)-C(4)	107.44(13)	O(32)-S(34)-C(34)	105.44(13)
O(1)-S(4)-C(4)	106.99(13)	O(31)-S(34)-C(34)	108.64(14)
N(4)-S(4)-C(4)	108.05(12)	N(34)-S(34)-C(34)	107.98(11)
C(7)-N(4)-S(4)	121.00(17)	C(37)-N(34)-S(34)	122.40(17)
N(4)-C(7)-C(11)	108.8(2)	N(34)-C(37)-C(41)	111.4(2)
N(4)-C(7)-C(8)	111.4(2)	N(34)-C(37)-C(38)	108.0(2)
C(11)-C(7)-C(8)	109.3(2)	C(41)-C(37)-C(38)	109.7(2)
C(9)-C(8)-C(10)	111.8(2)	C(39)-C(38)-C(40)	110.9(2)
C(9)-C(8)-C(7)	110.6(2)	C(39)-C(38)-C(37)	111.4(2)
C(10)-C(8)-C(7)	109.9(2)	C(40)-C(38)-C(37)	110.0(2)
O(11)-C(11)-N(11)	122.2(2)	O(41)-C(41)-N(41)	123.3(2)
O(11)-C(11)-C(7)	120.1(2)	O(41)-C(41)-C(37)	121.4(2)
N(11)-C(11)-C(7)	117.7(2)	N(41)-C(41)-C(37)	115.3(2)
C(11)-N(11)-C(12)	120.3(2)	C(41)-N(41)-C(42)	120.8(2)
N(11)-C(12)-C(13)	111.5(2)	N(41)-C(42)-C(43)	111.8(2)
N(13)-C(13)-C(14)	107.8(2)	N(43)-C(43)-C(44)	107.8(2)

N(13)-C(13)-C(12) 121.7(2)	N(43)-C(43)-C(42) 121.9(2)
C(14)-C(13)-C(12) 130.4(2)	C(44)-C(43)-C(42) 130.3(2)
N(15)-N(13)-C(13) 109.2(2)	N(45)-N(43)-C(43) 109.7(2)
N(14)-C(14)-C(13) 104.9(2)	N(44)-C(44)-C(43) 105.0(2)
N(15)-N(14)-C(14) 111.6(2)	C(44)-N(44)-N(45) 111.5(2)
N(15)-N(14)-C(15) 120.1(2)	N(45)-N(44)-C(45) 118.9(2)
C(14)-N(14)-C(15) 128.3(2)	C(44)-N(44)-C(45) 129.6(2)
N(14)-C(15)-C(16) 111.1(2)	N(44)-C(45)-C(46) 111.2(2)
N(13)-N(15)-N(14) 106.5(12)	N(43)-N(45)-N(44) 106.0(2)
N(16)-C(16)-C(17) 106.0(2)	N(46)-C(46)-C(47) 106.5(2)
N(16)-C(16)-C(15) 120.9(2)	N(46)-C(46)-C(45) 118.9(2)
C(17)-C(16)-C(15) 133.1(2)	C(47)-C(46)-C(45) 134.6(2)
O(16)-N(16)-C(16) 134.6(2)	O(46)-N(46)-C(46) 133.3(3)
O(16)-N(16)-O(17) 117.4(2)	O(46)-N(46)-O(47) 118.4(2)
C(16)-N(16)-O(17) 108.0(12)	C(46)-N(46)-O(47) 108.3(2)
N(17)-C(17)-C(16) 111.9(2)	N(47)-C(47)-C(46) 111.4(2)
N(17)-C(17)-C(18) 120.3(2)	N(47)-C(47)-C(48) 119.7(2)
C(16)-C(17)-C(18) 127.8(2)	C(46)-C(47)-C(48) 128.9(2)
C(17)-N(17)-O(17) 106.6(2)	C(47)-N(47)-O(47) 106.7(2)
N(17)-O(17)-N(16) 107.4(2)	N(47)-O(47)-N(46) 107.2(2)
C(19)-C(18)-C(23) 120.2(2)	C(53)-C(48)-C(49) 119.5(2)
C(19)-C(18)-C(17) 119.7(2)	C(49)-C(48)-C(47) 119.3(2)
C(23)-C(18)-C(17) 120.1(2)	C(53)-C(48)-C(47) 121.1(2)
C(20)-C(19)-C(18) 119.9(2)	C(50)-C(49)-C(48) 120.5(2)
C(21)-C(20)-C(19) 119.0(2)	C(49)-C(50)-C(51) 118.0(2)
C(20)-C(21)-C(22) 122.7(2)	C(52)-C(51)-C(50) 122.8(2)
C(20)-C(21)-N(21) 118.8(2)	C(50)-C(51)-N(51) 118.6(2)
C(22)-C(21)-N(21) 118.5(2)	C(52)-C(51)-N(51) 118.7(2)
C(21)-C(22)-C(23) 118.2(2)	C(51)-C(52)-C(53) 118.4(2)
C(22)-C(23)-C(18) 120.0(2)	C(52)-C(53)-C(48) 120.8(2)

O(21)-N(21)-O(22)	122.8(3)	O(51)-N(51)-O(52)	124.1(2)
O(21)-N(21)-C(21)	119.5(2)	O(51)-N(51)-C(51)	118.5(2)
O(22)-N(21)-C(21)	117.7(3)	O(52)-N(51)-C(51)	117.4(2)

References

1. Lizarzaburu, M. E.; Shuttleworth, S. J. 1,2,3,4-Tetrahydro-[gamma]-carbolinium salts: novel reactions with thiols, mediated by polymer-supported reagents. *Tetrahedron Letters* 2004, 45, 4781-4783.